Atmos. Chem. Phys., 17, 5623–5641, 2017
www.atmos-chem-phys.net/17/5623/2017/
doi:10.5194/acp-17-5623-2017

Atmospheric Chemistry and Physics
Open Access
EGU

Analysis of aerosol effects on warm clouds over the Yangtze River Delta from multi-sensor satellite observations

Yuqin Liu[1,2,3], Gerrit de Leeuw[1,3,4], Veli-Matti Kerminen[3], Jiahua Zhang[1], Putian Zhou[3], Wei Nie[5], Ximeng Qi[5], Juan Hong[3], Yonghong Wang[3], Aijun Ding[5], Huadong Guo[1], Olaf Krüger[3], Markku Kulmala[3], and Tuukka Petäjä[3]

[1]Institute of Remote Sensing and Digital Earth, Chinese Academy of Sciences, Beijing, China
[2]University of Chinese Academy of Sciences, Beijing, China
[3]Department of Physics, P.O. Box 64, 00014 University of Helsinki, Helsinki, Finland
[4]Finish Meteorological Institute, Climate Change Unit, P.O. Box 503, 00101 Helsinki, Finland
[5]Institute for Climate and Global Change Research & School of Atmospheric Sciences, Nanjing University, 210023 Nanjing, China

Correspondence to: Jiahua Zhang (zhangjh@radi.ac.cn)

Received: 10 November 2016 – Discussion started: 6 December 2016
Revised: 29 March 2017 – Accepted: 31 March 2017 – Published: 3 May 2017

Abstract. Aerosol effects on low warm clouds over the Yangtze River Delta (YRD, eastern China) are examined using co-located MODIS, CALIOP and CloudSat observations. By taking the vertical locations of aerosol and cloud layers into account, we use simultaneously observed aerosol and cloud data to investigate relationships between cloud properties and the amount of aerosol particles (using aerosol optical depth, AOD, as a proxy). Also, we investigate the impact of aerosol types on the variation of cloud properties with AOD. Finally, we explore how meteorological conditions affect these relationships using ERA-Interim reanalysis data. This study shows that the relation between cloud properties and AOD depends on the aerosol abundance, with a different behaviour for low and high AOD (i.e. AOD < 0.35 and AOD > 0.35). This applies to cloud droplet effective radius (CDR) and cloud fraction (CF), but not to cloud optical thickness (COT) and cloud top pressure (CTP). COT is found to decrease when AOD increases, which may be due to radiative effects and retrieval artefacts caused by absorbing aerosol. Conversely, CTP tends to increase with elevated AOD, indicating that the aerosol is not always prone to expand the vertical extension. It also shows that the COT–CDR and CWP (cloud liquid water path)–CDR relationships are not unique, but affected by atmospheric aerosol loading. Furthermore, separation of cases with either polluted dust or smoke aerosol shows that aerosol–cloud interaction (ACI) is stronger for clouds mixed with smoke aerosol than for clouds mixed with dust, which is ascribed to the higher absorption efficiency of smoke than dust. The variation of cloud properties with AOD is analysed for various relative humidity and boundary layer thermodynamic and dynamic conditions, showing that high relative humidity favours larger cloud droplet particles and increases cloud formation, irrespective of vertical or horizontal level. Stable atmospheric conditions enhance cloud cover horizontally. However, unstable atmospheric conditions favour thicker and higher clouds. Dynamically, upward motion of air parcels can also facilitate the formation of thicker and higher clouds. Overall, the present study provides an understanding of the impact of aerosols on cloud properties over the YRD. In addition to the amount of aerosol particles (or AOD), evidence is provided that aerosol types and ambient environmental conditions need to be considered to understand the observed relationships between cloud properties and AOD.

1 Introduction

Impacts of aerosols on clouds and precipitation have been reported as introducing the largest uncertainty in quantifying the anthropogenic contribution to climate change (Rosenfeld, 2000; Twomey, 1974; Gryspeerdt et al., 2014; Kaufman et al., 2012). Atmospheric aerosol particles have been recognized as having two effects on Earth's climate. First, they can

directly alter the energy balance due to scattering and absorption of incoming solar radiation (e.g. McCormick and Ludwig, 1967). Second, they can act as cloud condensation nuclei (CCN) and thus modify the cloud micro-physical properties and lifetime as well as precipitation (Ramanathan et al., 2001; Krüger and Grassl, 2011). The effects of aerosol-induced changes of cloud properties on the radiation budget are collectively referred to as the aerosol indirect effect (AIE). The study presented here is confined to aerosol–cloud interaction (ACI) using satellite data.

The activation of aerosol particles to CCN, or more specifically the number concentration of CCN, is a direct link between aerosols and clouds, and the aerosol activation efficiency is a key aerosol property affecting ACI. For a given constant cloud liquid-water path (CWP), an increased aerosol loading is expected to lead to smaller and more numerous cloud droplets, resulting in an increase of cloud albedo. This process, termed as the "first AIE" or "Twomey's effect", may lead to a net cooling of climate (Twomey, 1974; Feingold et al., 2003). The reduced cloud droplet effective radius (CDR) also suppresses precipitation and can consequently increase cloud lifetime, thus maintaining a larger liquid-water path, with a possible further increase in the cloud optical thickness (COT) and cloud reflectance. This process, described as the "second AIE", may further influence the cloud fraction (CF) (Albrecht, 1989; Feingold et al., 2001). The interaction mechanisms between aerosols and clouds remain among the most uncertain processes in the global climate system in spite of a large number of studies made using both observations (Platnick et al., 2003; Koren et al., 2005; Krüger et al., 2004) and models (Suzuki et al., 2004; Quaas et al., 2009; Sena et al., 2016).

In order to better understand aerosol indirect effects, we resorted to statistical analysis of satellite observations. By virtue of their large coverage and high spatial and temporal resolution, satellite-borne instruments have become a promising observational tool in studying ACIs. Previous studies using a large amount of satellite data and/or multiple satellite instruments have shown that aerosol particles can affect cloud properties significantly (Krüger and Grassl, 2002; Menon et al., 2008; Sporre et al., 2014; Rosenfeld et al., 2014; Saponaro et al., 2017). Satellite measurements suggest that the CDR tends to decrease with increasing aerosol loading, which is consistent with Twomey's theory (Matheson et al., 2005; Meskhidze and Nenes, 2010; Koren et al., 2005). However, positive correlations between CDR and aerosol optical depth (AOD) have also been found in some study areas, from both observations and models, especially over land (Feingold et al., 2001; Grandey and Stier, 2010; Yuan et al., 2008). Different behaviours of CDR as a function of AOD for different AOD regimes (low or high) have been observed by, for example, Tang et al. (2014) and Wang et al. (2015). Feingold et al. (2001) concluded that there are three kinds of CDR responses to aerosol enhancement: the CDR decreases with increasing aerosol loading followed by (1) a saturation of the value of CDR in response to high AOD, (2) a decrease in the CDR with further increasing AOD due to suppression of cloud water vapour supersaturation caused by abundant large particles, or (3) an increase in CDR with further increases in AOD due to an intense competition for vapour which evaporates the smallest droplets. Likewise, the aerosol impact on COT is still poorly quantified. Costantino and Bréon (2013) reported that the relationship between AOD and COT, which can be either positive or negative, depends on the balance between the simultaneous CDR increase and CWP decrease when AOD increases. With regard to the impact of aerosols on the cloud life cycle, it is of great importance to explore the relationship between the aerosol loading and cloud fraction, because the cloud fraction is highly associated with other cloud properties and has a large effect on radiation (Gryspeerdt et al., 2016). Kaufman and Koren (2006) and Koren et al. (2008) reported an increase in the cloud cover with an increasing aerosol loading, followed by an inverse pattern due to the absorption efficiency of aerosol. This brief summary shows that the aerosol effect on cloud properties and the magnitude of this effect are still very unclear.

Aerosol and cloud properties may have different vertical distributions and may actually not physically interact. Costantino and Bréon (2013) and Jones et al. (2009), using MODIS data, found that the aerosol indirect effect is stronger for well-mixed clouds than for well-separated clouds (in well-mixed aerosol and cloud, layers are physically interacting, as further explained in Sect. 2). These observations show that it is important to consider the relative altitudes of aerosol and cloud layers when estimating the aerosol indirect effects. In addition, local differences in aerosol populations and cloud regimes may have a strong effect on ACI (Sinha et al., 2003; Small et al., 2011; Kaufman et al., 2005). Yuan et al. (2008) proposed that the chemical composition of aerosol particles may play a role in determining the relationship between AOD and CDR. Meteorology can affect the interaction between aerosol and cloud, which usually further complicates ACI (Koren et al., 2010; Reutter et al., 2009; Loeb and Schuster, 2008; Su et al., 2010; Stathopoulos et al., 2017). As a consequence, the widely varying estimates of the aerosol impact on cloud parameters, either positive or negative, depend on factors like the aerosol size distribution and chemical composition, cloud regime, and local meteorological conditions. Therefore, the dataset used in this study contains not only aerosol and cloud properties derived from MODIS, CALIOP and CloudSat, but also the meteorological parameters collected from the daily ERA-Interim reanalysis data.

The Yangtze River Delta (YRD) is characterized by a variable aerosol composition and increasing aerosol concentration during the last two decades (Ding et al., 2013a; Qi et al., 2015). Using multi-sensor retrievals, this study aims to systematically examine the response of warm cloud parameters (CDR, CF, COT and CTP) to the increase in the aerosol loading, where AOD is used as a proxy for CCN number con-

centration (Andreae, 2009; Kourtidis et al., 2015). New insights into the changing cloud properties over a wide range of aerosol loadings, in particular in high AOD conditions, result from our focus on a systematic understanding of ACI from three perspectives: (1) well-mixed and well-separated clouds, (2) aerosol effects on properties of well-mixed clouds and (3) well-mixed clouds under different meteorological conditions.

The paper is organized as follows: Sect. 2 describes the datasets used, data processing and the main analysis conducted to explore aerosol cloud interaction. Section 3 starts with a general description of aerosol and cloud properties and the effect of aerosol loading on the relations between them, followed by a description of aerosol effects on cloud properties (CDR, CF, COT and CTP). In the latter we discriminate between well-separated and well-mixed clouds. The focus will be on well-mixed clouds where ACI takes place, and aerosol types and meteorological factors are considered to better understand the possible mechanisms. Overall conclusions and discussions are presented in Sect. 4.

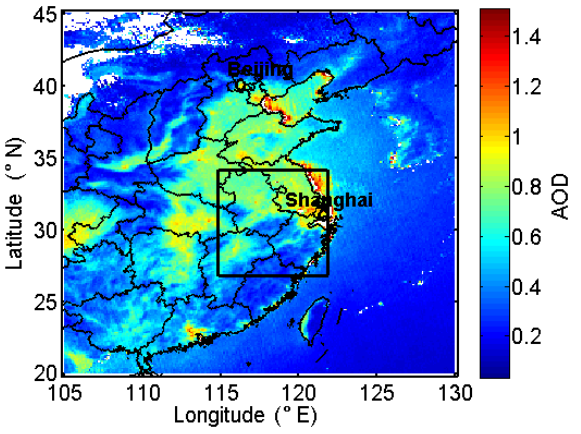

Figure 1. Map of annual averaged MODIS/AQUA level 2 AOD for all years during the period from 2007 to 2010. The black rectangle (27–34° N and 115–122° E) indicates the Yangtze River Delta (YRD).

2 Methods

2.1 Description of the study region

In this study, the YRD, covering the area 27–34° N and 115–122° E (Fig. 1), was chosen in order to investigate the aerosol-induced variability in micro- and macro-physical properties of low warm clouds during 4 consecutive years (2007–2010). The YRD region was chosen because it is representative of the continental East Asian subtropical climate. The marine monsoon subtropical climate for YRD is characterized by hot and humid summers and cool dry winters (Sundström et al., 2012; Zhang et al., 2010). The mean temperature in summer is about 27–28 °C. Mean annual precipitation ranges from 1000 to 1400 mm and most precipitation occurs in spring and summer (Zhang et al., 2010; Cao et al., 2016).

The population density in the YRD is very high with intensive human activities in the region contributing to a very variable and complex aerosol composition. The YRD has been reported as a major source region of both black carbon and sulfate (Wang et al., 2014; Andersson et al., 2015). In addition, other aerosol sources such as dust emissions render the interactions between aerosols and clouds complicated (Nie et al., 2014). The continental area of interest is characterized by a high level of anthropogenic emissions and is well suited for research related to the indirect effects of aerosols on cloud micro- and macro-physical properties.

2.2 Data sources

The MODIS sensor, on board the Aqua satellite, has a swath width of ∼ 2300 km and multi-band spectral coverage (King et al., 2003). The MODIS/Aqua overpass time for the study area is around 13:30 LT (local time), when continental warm clouds are likely to be well developed. Therefore MODIS/Aqua was selected as a data source to explore the ACI over this area. In this work, we used the MODIS Collection 5.1 AOD product (MOD04) derived from cloud-free pixels (resolution 500 m at nadir) and aggregated to a resolution of 10 km × 10 km (Remer et al., 2005; Levy et al., 2010). The AOD over land is retrieved using three MODIS channels: 0.47, 0.66 and 2.13 µm (Remer et al., 2005). Cloud properties are retrieved using six spectral channels (King et al., 1997) at visible and near-infrared wavelengths (i.e., 0.66, 0.86, 1.24, 1.64, 2.12 and 3.75 µm). Here, we used the AOD as a proxy for aerosol burden in our ACI analysis. The cloud properties used in this study, CDR, CWP, COT, cloud top pressure (CTP) and cloud phase infrared (CPI), were obtained from the Level 2 cloud product (MYD06) (King et al., 2003). Both these products, MOD04 and MYD06, are in good agreement with ground-based remote sensing data (Levy et al., 2010; Platnick et al., 2003). More detailed information on algorithms for the retrieval of aerosol and cloud properties is provided at http://modis-atmos.gsfc.nasa.gov.

Along with the Aqua satellites, CloudSat and CALIPSO (Cloud–Aerosol Lidar and Infrared Pathfinder Satellite Observations) are flying in the so-called "A-train" constellation together with other NASA satellites (Stephens et al., 2002). CloudSat carries the CPR (cloud profiling radar), i.e. the first satellite-based millimetre-wavelength cloud radar to detect the vertical information on different-sized cloud droplets (Im et al., 2005). The CPR is able to penetrate optically thick clouds and detect weak precipitating particles (Wang et al., 2013). In the present study we utilized the datasets CloudLayerBase and CloudLayerTop from 2B-CLDCLASS-LIDAR, the latest version (R04) of the CloudSat standard data products. The data are provided in the CPR spatial grid with vertical and horizontal resolu-

tions of approximately 480 m and 1.4 × 1.8 km, respectively. CALIOP (Cloud–Aerosol Lidar with Orthogonal Polarization) on board CALIPSO is the first space-borne near-nadir polarization lidar optimized for aerosol and cloud measurements (Winker et al., 2003). It is sensitive to optically thin clouds which could be missed by CPR (Wang et al., 2013). The datasets Layer_Base_Altitude and Layer_Top_Altitude retrieved from the CALIOP level-2 aerosol layer product (05kmALay) were used in the present study. Its footprint is very narrow, with a laser pulse diameter of 70 m on the ground. The vertical resolution of the CALIOP layer product varies with altitude: 30 m for $h = 0$–8.2 km, 60 m for $h = 8.2$–20.2 km and 180 m for $h =$ 20.2–30.1 km, whereas the horizontal resolution is 5 km (Liu et al., 2009). Combining CloudSat and CALIPSO observations has provided new insights into the vertical structure and micro-physical properties of clouds (Matrosov, 2007).

The daily temperature at the 1000 and 700 hPa levels, relative humidity at the 950 hPa level and pressure vertical velocity (PVV) at the 750 hPa level were obtained from ERA-Interim reanalysis data. The daily ERA-Interim reanalysis contains global meteorological conditions with 0.125° × 0.125° grids and a 37-level vertical resolution (1000–01 hPa) every 6 h (00:00, 06:00, 12:00, 18:00 UTC) (http://apps.ecmwf.int/datasets/data/interim-full-daily/). The reanalysis data were used for the closest collocation with the satellite overpass time over the study area.

2.3 Data processing

The MODIS/AQUA, CALIOP/CALIPSO and CPR/CloudSat satellites are part of the A-Train constellation and observe the same scene on Earth within 1–2 min (Stephens et al., 2002). Therefore, time coincidence of retrievals is assured when the datasets are extracted for the same date. Meteorological properties retrieved from the 06:00 UTC ERA-Interim datasets were used here as the "A-train" satellites constellation overpasses the region of interest at about 13:30 LT (05:30 UTC). We aggregated CDR, COT and CWP (1 km × 1 km) to a resolution of 5 km × 5 km to match the along-track resolution of CALIOP (5 km × 5 km), while CTP, CF and CPI were directly applied for the analysis since all of them are at a 5 km × 5 km spatial resolution.

Aerosol properties are only retrieved for strictly cloud-free pixels as determined by the application of a cloud-detection scheme. However, cloud detection schemes are not perfect and some residual clouds may remain undetected resulting in high AOD (Kaufman et al., 2005). Another potential source of error could be the misclassification of high AOD areas, such as in the presence of desert dust or very high pollution levels, as clouds. To reduce a possible over-estimation of AOD, cases with AOD greater than 1.5 were excluded from further analysis. In this paper, we focused on warm clouds with CTP larger than 700 hPa and CWP lower than 200 g m^{-2}, as most aerosols exist in the lower troposphere (Michibata et al., 2014). In addition, only cases with CPI = 1 (liquid-water cloud) were included. When CALIOP detected the presence of aerosol, we averaged the MODIS aerosol retrievals within a radius of 50 km from the CALIOP target. Likewise, we averaged the MODIS cloud retrievals within a radius of 5 km from the CALIOP target. For meteorological properties, we chose the value of the footprint that is nearest to the CALIOP target. MODIS, CALIOP and CPR datasets are listed in Table 1.

A quantitative relationship between AOD and cloud properties has been documented in previous studies (Sporre et al., 2014; Meskhidze and Nenes, 2010; Koren et al., 2005, Saponaro et al., 2017). However, the relative vertical positions of aerosol and cloud layers contribute to the uncertainty in this relationship. Following the method by Costantino and Bréon (2013), we considered the aerosol and cloud layers to be physically interacting (well mixed) when the vertical distance between bottom (top) of the aerosol layer and the top (bottom) of a cloud layer was smaller than 100 m. Coincident samples with a vertical distance larger than 750 m were assumed to be "well separated". Coincident samples with a distance between 100 and 750 m were defined as "uncertain". The uncertain cases, as identified using the information from CloudSat, were excluded from further analysis in this study. Cloud types were identified as single-, double- and multi-layer clouds using the cloud layer information at each point. Single-, double- and multi-layer cloud samples accounted for 59, 30 and 11 % of the total samples, respectively. Using the highest occurrence frequency (OF) of aerosol type below 10 km altitude at each point, the aerosol type of highest OF was defined following the Feature_Classification_Flags derived from CALIOP.

Meteorological and aerosol impacts on cloud macrophysics and micro-physics are found to be tightly intermingled (Stevens and Feingold, 2009). In an attempt to isolate aerosol effects, the meteorological effects on clouds were explored in a statistical sense. Meteorological properties used here include relative humidity, lower tropospheric stability (LTS) and PVV. LTS is defined as the difference in potential temperature between the free troposphere (700 hpa) and the surface, which is representative of typical thermodynamic conditions (Klein and Hartmanm, 1993). It has been suggested that relative humidity, LTS and PVV affect aerosol and cloud interaction (Gryspeerdt et al., 2014; Small et al., 2011). A positive LTS is associated with a stable atmosphere in which vertical mixing is prohibited; negative PVV indicates a local upward motion of air parcels.

Table 1. Level 2 MODIS, CALIOP, CALIOP/CPR and ERA-Interim products used to characterize aerosol and cloud properties.

Product	Dataset	Horizontal resolution	Data source
Aerosol (MYD04 Level 2 Collection 5)	Optical_Depth_Land_And_Ocean	10 km	MODIS
Cloud (MYD06 Level 2 Collection 5)	Cloud_Effective_Radius	1 km	
	Cloud_Water_Path	1 km	
	Cloud_Phase_Infrared_Day	5 km	
	Cloud_TOP_Pressure_Day	5 km	
	Cloud_Fraction_Day	5 km	
	Cloud_Optical_Thickness	1 km	
Cloud (2B-CLDCLASS-LIDAR)	CloudLayerBase	2.5 km	CALIOP/CPR
	CloudLayerTop	2.5 km	
Aerosol (05kmALay)	Layer_Top_Altitude	5 km	CALIOP
	Layer_Base_Altitude	5 km	
	Cloud_Aerosol_Discrimination	5 km	
	Feature_Classification_Flags	5 km	
ERA-Interim	Temperature (700, 1000 hPa)	0.125°	ECMWF
	Relative humidity (950 hPa)	0.125°	
	Pressure vertical velocity (750 hPa)	0.125°	

3 Results and discussions

3.1 Overall aerosol and cloud characteristics

3.1.1 Spatial and time-series analysis of aerosol and cloud parameters

The spatial variations of the aerosol and cloud properties over the study area, averaged over the years 2007–2010, are shown in Fig. 2. We can see a decreasing north–south pattern in AOD in Fig. 2a, with the highest values found in the north-east area. CDR behaves similarly to AOD, except that the highest values are found in the northernmost area. Contrary to AOD, both COT and CWP show an increasing north–south pattern. Furthermore, the spatial distributions of COT and CWP are remarkably similar to each other.

Figure 3 shows time series of the monthly-averaged values for the AOD, CDR, COT, CWP, CF and CTP, calculated for each month during the four years 2007–2010. Both the monthly-averaged AOD and CDR are highest in June. December presents the lowest monthly average for the AOD. Overall, the variations of the monthly-averaged COT and CWP are similar, with the lower values in the summer and the higher values in the winter. The monthly-averaged CF approaches its maximum values in January and June, while CTP shows two peaks in February and September. Note that CTP is plotted along the vertical axis from high to low. The monthly averages are determined from the numbers of samples presented in Table 2 for each parameter and each month between 2007 and 2010. Further, the availabilities of data for AOD and cloud properties are not the same for the whole acquisition period between 2007 and 2010. It indicates that not every CALIPSO shot has all the corresponding value for AOD, CDR, COT, CWP, CF or CTP, which will decrease the data sample size to some extent.

3.1.2 Variation of COT and CWP with CDR

Prior to investigating the aerosol impact on warm cloud properties, a general analysis of cloud properties and the effect of aerosol loading on the relations between them are discussed below. The overall statistical relations between the cloud parameters used in this study are derived from the scatter plots shown in Fig. 4. All CDR, COT, CTP and CWP data shown in Fig. 4 (and later figures) are averaged over AOD bins, from 0.05 to 1.5 with a step of 0.02 on a log–log scale. Student's t test is used to determine whether two sets of data are significantly different from each other. The p value is defined as the probability of obtaining a result equal to or "more extreme" than what was actually observed, when the null hypothesis is true. The marker $*$ at the top right corner of R value denotes statistically significant if $p < 0.05$.

We first explored the response of CDR to the increasing AOD in mixed aerosol–cloud layers and found that CDR decreases with increasing AOD in moderately polluted conditions (AOD < 0.35). In polluted and heavily polluted conditions (AOD > 0.35), however, CDR increases with increasing AOD. Here we discriminate between moderately polluted (AOD < 0.35), polluted (AOD >= 0.35 and AOD <= 0.8) and heavily polluted (AOD > 0.8) conditions. The threshold of 0.35 for AOD is chosen based on analysis presented below in Sect. 3.2, where we compare the relation of cloud parameters and AOD in more detail. Figure 4a shows a scatter plot of COT versus CDR for well-mixed clouds. The correlation between these parameters is negative, i.e. COT decreases with CDR, with a correlation coefficient equal to −0.47. Figure 4c shows the same data but a distinction is made between data

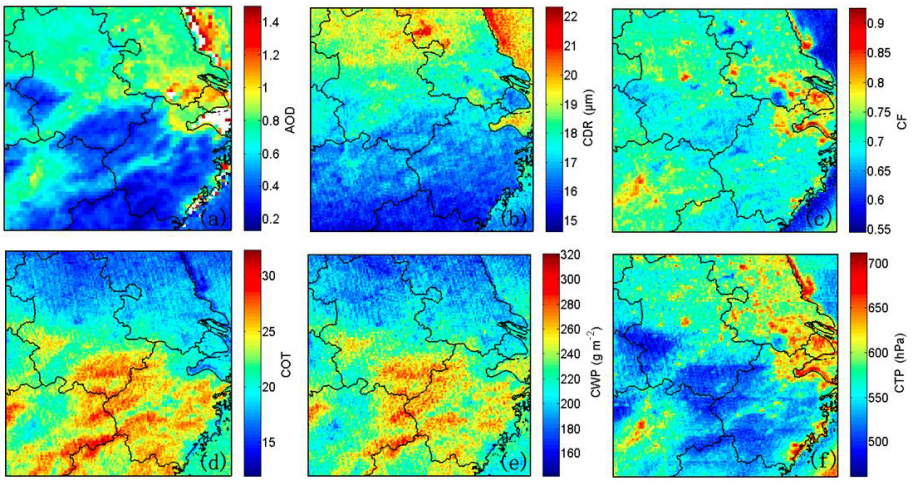

Figure 2. Spatial distributions of AOD **(a)**, CDR **(b)**, CF **(c)**, COT **(d)**, CWP **(e)** and CTP **(f)** averaged over all years between 2007 and 2010.

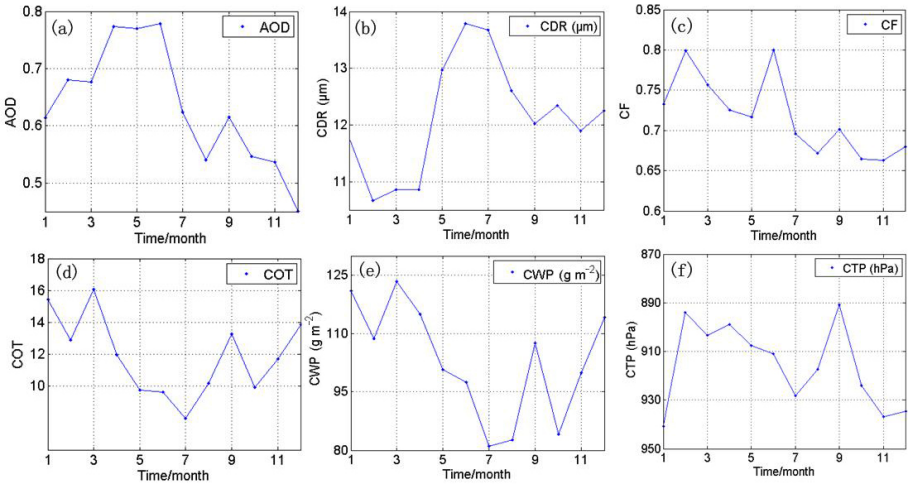

Figure 3. Time series of the monthly-averaged values of AOD **(a)**, CDR **(b)**, CF **(c)**, COT **(d)**, CWP **(e)** and CTP **(f)** for the dataset of MODIS–CALIPSO coincidences for all months between 2007 and 2010. Month 1 is January.

points in moderately polluted, polluted and heavily polluted conditions. For this dataset, COT increases with an increasing CDR at moderately polluted conditions. In contrast, for heavily polluted conditions COT shows a decrease with an increasing CDR. This may indicate the existence of intense competition between the aerosol particles for water vapour where the larger droplets are more prone to condensation of water vapour than smaller ones, and thus grow to larger sizes. This results in a shift of the droplet spectrum to larger sizes due to the increase of CDR accompanied by a decrease of COT (Wang et al., 2015). The data for the three different AOD cases show that the relationship between CDR and COT is not unique and depends on the aerosol abundance. Costantino and Bréon (2013) compared the CDR–COT relationship of mixed and separated aerosol–cloud layers and found an increase in the CDR with increasing COT, followed by a decrease with higher COT in both cases (mixed and separated aerosol–cloud layers). Compared to their study, we consider the effect of aerosol loading on the relationship between CDR and COT in both cases.

Figure 4b shows a weak correlation between CWP and CDR for well-mixed cloud layers, with a correlation coefficient equal to -0.15. However, when different degrees of pollution are considered (Fig. 4d), we see a clear correlation between both parameters ($R = 0.78$) in moderately polluted conditions, where CWP clearly increases with increasing CDR. In polluted and heavily polluted conditions the variation of CWP with increasing CDR is much weaker ($R = 0.31$ for polluted conditions) and in heavily polluted conditions CWP decreases with increasing CDR ($R = -0.33$).

Table 2. The sample sizes of all months for each parameter.

Parameters	January	February	March	April	May	June	July	August	September	October	November	December	Total
AOD	5428	3332	3892	4704	5598	3638	5944	6630	4306	6728	6110	6400	62 710
CDR	794	669	365	679	714	872	1228	2013	1514	1281	895	582	11 606
COT	886	747	392	732	748	915	1298	2072	1539	1329	967	627	12 232
CWP	1226	1125	620	1310	1226	1245	1490	2187	1929	1715	1261	867	16 201
CF	1398	994	537	955	993	1065	1671	2650	1996	1811	1373	1119	16 562
CTP	1398	994	537	955	993	1065	1671	2650	1996	1811	1373	1119	16 562

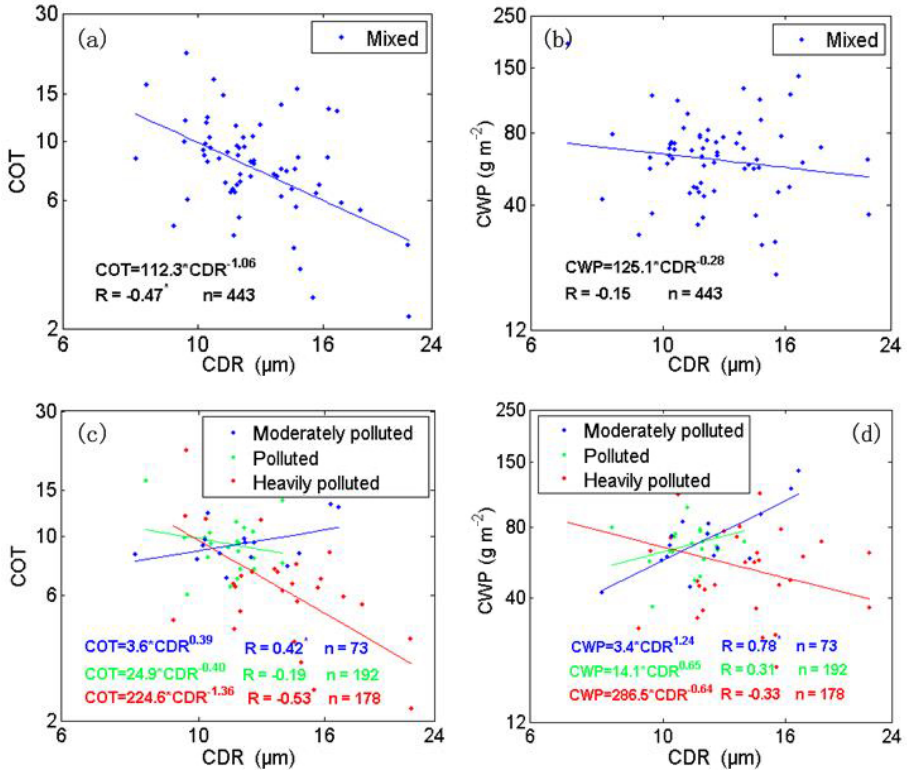

Figure 4. Scatter plots of cloud parameters versus CDR in well-mixed aerosol–cloud layers: **(a)** COT and **(b)** CWP, both for all data; **(c)** COT and **(d)** CWP, both for data grouped by moderately polluted (in blue), polluted (in green) and heavily polluted (in red) atmospheric conditions. Here moderately polluted refers to AOD < 0.35, polluted refers to 0.35 <= AOD <= 0.8 and heavily polluted refers to AOD > 0.8. The lines present the least-square fits, and the resulting relations are presented in each figure. The number of data samples is also reported in the figure (and following figures).

3.1.3 Variation of COT and CWP with cloud top height

CTP is generally used as a measure of cloud top height (CTH), with higher CTP implying a lower CTH. Figure 5a shows a positive correlation between CTP and COT, implying the occurrence of higher clouds with an increasing COT, which is consistent with the general understanding of ACIs. Note that here and in the following figures, CTP is plotted along the vertical axis from high to low, i.e. decreasing CTP indicates increasing CTH, and positive correlations between CTP and other cloud parameters indicate that an increase in these parameters corresponds to a higher CTH. Figure 5b shows a positive correlation between CTP and CWP, which again implies that clouds are higher as CWP increases. An explanation for this phenomenon is provided by Gao et al. (2014), i.e. clouds grow in the vertical and more drizzle is produced, so that the CWP becomes larger. Figure 5c shows the relation between CWP and COT. The CWP increases with the increase of COT, which is in good agreement with the aerosol second indirect effect hypothesis that the precipitation suppression can increase CWP and possibly further increase COT. This observation is in good agreement with those of Costantino and Bréon (2013) that cloud water amount increases with increasing COT.

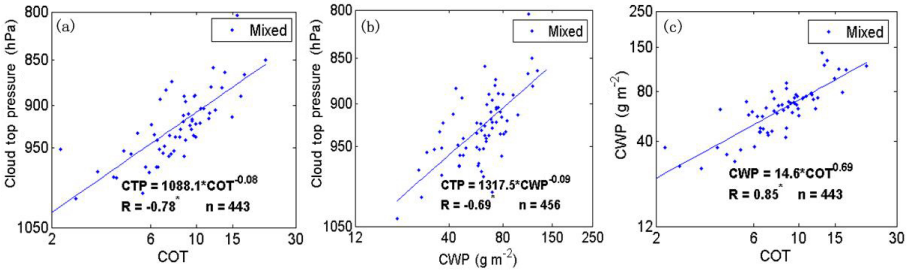

Figure 5. Scatter plots of cloud parameters in well-mixed aerosol cloud layers for all data: **(a)** CTP versus COT, **(b)** CTP versus CWP, and **(c)** CWP versus COT. The lines present the least-square fits, and the resulting relations are presented in each figure.

3.2 Difference between separated and mixed conditions

In this section we examine the responses of various cloud properties to the increasing AOD for well-separated and well-mixed clouds, respectively. Figure 6 shows relations between cloud parameters (CDR, CF, COT, CTP) and AOD for both separated and mixed conditions. The strength of the interaction between cloud properties and AOD is quantified here as the slope of the line describing the relation between cloud parameters and AOD, on a log–log scale, as obtained by linear regression. In Fig. 6a, CDR shows a negative relation with AOD in moderately polluted conditions when aerosol and cloud layers are mixed, which is in good agreement with Twomey's theory (Twomey, 1977). We note that, due to the limited number of data points in the dataset with AOD < 0.35, the present work does not allow the selection of conditions with a constant CWP. Following, for example, Costantino and Bréon (2010, 2013) and Wang et al. (2015), we use all available data together. In polluted and heavily polluted conditions, however, CDR increases with increasing AOD, suggesting some sort of saturation in ACIs when AOD approaches 0.35. This value for the tipping point (0.35) is close to the value of 0.4 reported by Feingold et al. (2001). As discussed earlier, Feingold et al. (2001) proposed three primary responses of CDR to the aerosol loading. We consider the fact that CDR increases with an increase in AOD when AOD loading exceeds 0.35 as the "anti-Twomey effect". The positive relation between CDR and AOD may be similar to that described by Feingold et al. (2001), case 3 (see above), i.e. due to intense vapour competition the smaller droplets evaporate as the number of particles continues to increase. It may also be that only a subset of aerosol particles is activated when not enough vapour is available, and once activated they continue to grow faster, thus preventing water vapour from condensing onto smaller aerosol particles that are less susceptible to activation, resulting in the increase of CDR.

Figure 6a also shows that, in well-separated cloud layers, CDR varies much less with AOD irrespective of whether the AOD is relatively low or high. Such a weaker variation can be attributed to the fact that no aerosols are subjected to cloud micro-physical process since there are no physical interactions between aerosol and cloud layers.

Figure 6b shows that when aerosol and cloud layers physically interact, the CF shows a decrease with an increasing AOD in moderately polluted conditions, albeit with a low significance as indicated by the small correlation coefficient R, followed by an inverse pattern in polluted and heavily polluted conditions. This outcome is not in agreement with the findings of Koren et al. (2008) and Small et al. (2011). It could be explained as follows: here, when aerosol and cloud layers are well-mixed, the absorption of solar radiation heats the mixed layer and reduces the cloud cover due to the quite high concentrations of the smoke particles over the YRD. This feedback would be balanced once the heating of the surface raises the surface temperature. It destabilizes the atmosphere, resulting in vertical transport and thus enabling transfer of humidity from the surface to higher levels in the atmosphere. This effect increases cloudiness (Koren et al., 2008). Conversely, CF shows an increasing pattern with an increasing AOD for the whole AOD dataset in well-separated cloud layers. This increase might be due to absorbing aerosols interacting with incoming solar radiation above the cloud layer (Costantino and Bréon, 2013). In this process, absorbing aerosols above cloud tops may heat the aerosol layer and cool the surface, thereby stabilizing the boundary layer and maintaining a moist boundary layer. In addition, scattering aerosol reduces the amount of solar light reaching the surface. This combination of two effects suppresses cloud vertical development and increases the low cloud cover.

The COT has a negative correlation with AOD in both conditions, as shown in Fig. 6c. There are two effects that may contribute to this negative relationship. On the one hand, the evaporation of cloud droplets caused by locally absorbing aerosol makes clouds thinner, which is a radiative effect. On the other hand, the presence of absorbing aerosol may influence the satellite-retrieved COT because it can absorb radiation and thus reduce the cloud reflectance measured by the sensors on the satellite (Meyer et al., 2013, 2015; Li et al., 2014; Ten Hoeve et al., 2011). Meyer et al. (2013) reported that adjusting for above-cloud aerosol attenuation can increase the retrieved regional mean COT by roughly 18 %

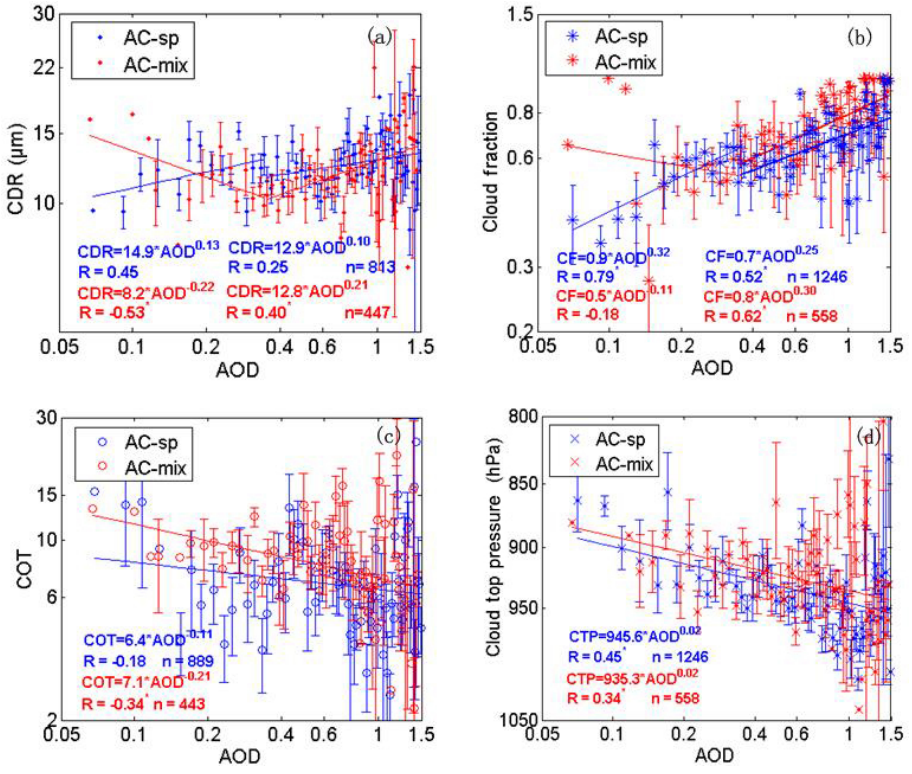

Figure 6. Scatter plots of cloud parameters versus AOD over YRD on log–log scale for cases of separated (blue) and mixed (red) aerosol–cloud layers: **(a)** CDR versus AOD, **(b)** CF versus AOD, **(c)** COT versus AOD and **(d)** CTP versus AOD. The lines present the least-square fits, and the resulting relations are presented in each figure. Error bars represent the confidence level of the mean cloud parameters' value for each AOD bin, i.e. the statistical uncertainties, expressed as $\sigma/(n-2)$, where n is the number of cases within the AOD bin and σ is the standard deviation of cloud properties.

for polluted marine boundary layer clouds. Li et al. (2014) also found that, due to absorbing aerosols in the heart of the YRD region, satellite observations tend to underestimate COT. The radiative effect and retrieval uncertainty could be the important factors for the decrease of COT with increasing AOD, as suggested by Ten Hoeve et al. (2011) and Alam et al. (2014). These authors reported similar results on the decrease of COT with increasing AOD, which may result from the measured reflectance from a cloud top at visible wavelengths being smaller than expected due to absorbing aerosols.

The relationship between CTP and AOD has been plotted in Fig. 6d. There is a positive correlation between CTP and AOD, which is contradicting the general understanding that high aerosol loading will result in an increase of cloud lifetime and higher cloud top. The positive relation between CTP and AOD has an implication that higher aerosol abundance is not always accompanied by smaller CTP. This suggests that the primary effect of aerosol is not always to produce taller and more convective clouds (Rennóet al., 2013).

Based on the above findings, we conclude that for well-mixed clouds in the YRD, the CDR shows a decrease with an increasing AOD under moderately polluted conditions, followed by an increase under polluted and heavily polluted conditions due to the intense water vapour competition. The cloud cover behaves qualitatively similar to CDR in response to changing values of AOD. Meanwhile, cloud optical depth becomes smaller and CTP becomes larger with increasing AOD over the whole range of AOD values.

3.3 Case of mixed aerosol–cloud layers

3.3.1 ACI for single-layer mixed clouds

Well-mixed clouds show a stronger relation between aerosol and cloud properties than separated clouds, as shown above. From here on, we will focus on potential aerosol indirect effects on well-mixed warm clouds as defined above. Relations between CDR, CF, COT and CTP with AOD will be explored in this section. Figure 7 shows the variation of single-layer cloud properties with AOD when aerosol and cloud layers are mixed. The relation between CDR and AOD changes from negative for AOD < 0.35 to positive for AOD > 0.35 (Fig. 7a). As with the CDR, the CF shows similar variation with the elevated AOD over the whole AOD range. Figure 7c shows that COT is negatively associated with increasing AOD. In contrast, CTP decreases with increasing AOD (Fig. 7d), i.e.

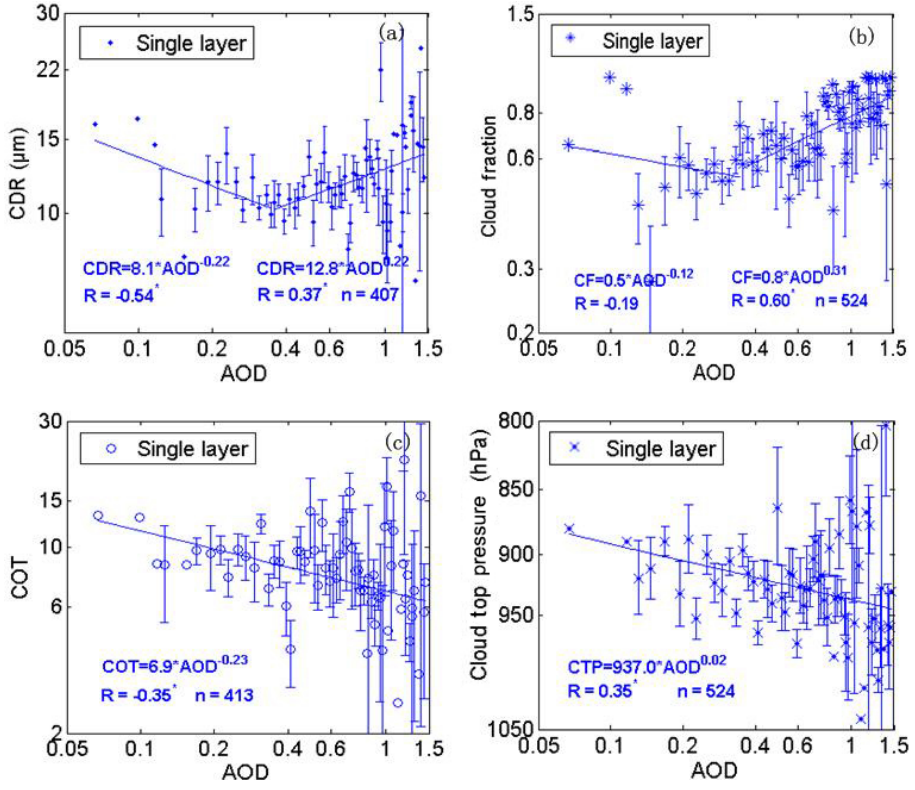

Figure 7. Scatter plots of cloud parameters versus AOD over YRD on log–log scale for mixed-aerosol single-layer clouds: **(a)** CDR, **(b)** CF, **(c)** COT and **(d)** CTP. The lines present the least-square fits, and the resulting relations are presented in each figure. The error bars indicate the statistical uncertainties as in Fig. 6.

CTH increases. In general, the characteristics for cases of mixed-aerosol single-layer warm clouds (Fig. 7) are quite similar to the case of mixed-aerosol warm clouds (Fig. 6). The slight difference of fits comes from the different types of clouds that are considered in different conditions. In Fig. 6, the clouds are not limited to single-layer warm clouds, but also double-layer warm clouds.

3.3.2 Influence of aerosol type on ACI

Eastern China is a region with high concentrations of sulfate, dust, black carbon and other carbonaceous aerosols. In heavily polluted areas, dust aerosols become coated with hygroscopic material, making them effective CCN (Levin et al., 1996; Satheesh et al., 2006). In particular, there are high emissions of smoke by straw-burning in summertime. ACI is strongly dependent on the aerosol types, their size distribution and the vertical variation of these, as well as ambient environmental conditions (Patra et al., 2005; Matsui et al., 2006; Dusek et al., 2008; Yuan et al., 2008). Thus, aerosol species are indicative of causal micro-physical and radiative effects. Different aerosol types may reveal different patterns of ACI. Here, polluted dust (accounting for 34 %) and smoke aerosol (accounting for 38 %), which are the two main aerosol types occurring in the YRD, are chosen to investigate the variation of cloud parameters with AOD. Smoke (fine absorbing particles) and polluted dust (coarse particles) aerosols are identified using the CALIOP classification. In addition, they have different efficiency for the absorption of sunlight.

Figure 8 shows the variation of cloud parameters with AOD over the YRD, where data points for mixed polluted dust-warm clouds and mixed-smoke-aerosol warm clouds are indicated with different colours. Figure 8a shows that the CDR is, in general, larger in the presence of smoke aerosol than in the presence of dust. Meanwhile, the cloud fraction is smaller in the presence of smoke, as shown in Fig. 8b. This can be due to the greater efficiency of smoke aerosol particles for the absorption of sunlight than that of dust, resulting in local warming in the presence of smoke aerosol which in turn leads to evaporation of water and thus an increase in small droplets or even complete evaporation of cloud droplets and thus a reduction of cloud cover. Figure 8c shows that the COT decreases with increasing AOD for both aerosol types albeit with a low significance as indicated by the small correlation coefficient R. The slope of linear regression of COT against AOD is much stronger in the presence of smoke aerosol than in the presence of dust, indicating that the ACI is stronger for smoke than for polluted dust. In addition to those men-

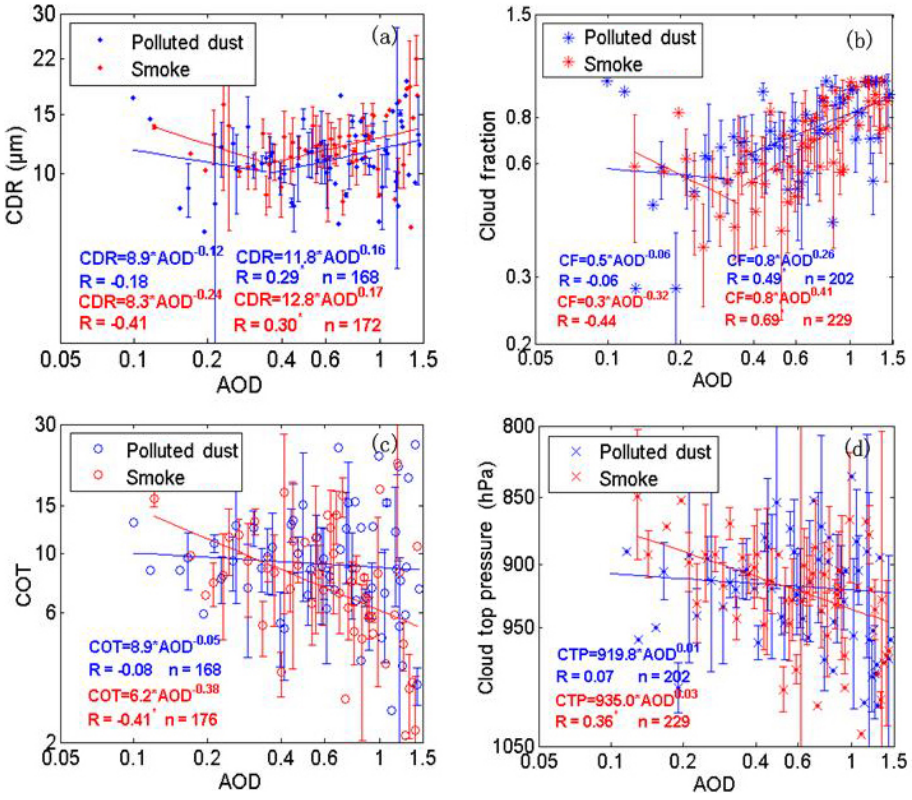

Figure 8. Scatter plots of cloud parameters versus AOD over YRD on log–log scale for cases of mixed-dust-aerosol cloud layers (blue) and mixed-smoke-aerosol cloud layers (red): **(a)** CDR, **(b)** CF, **(c)** COT and **(d)** CTP. The lines present the least-square fits, and the resulting relations are presented in each figure. The error bars indicate the statistical uncertainties as in Fig. 6.

tioned, one factor which probably also contributes to the observed difference between effects of smoke and polluted dust is that dust does not absorb sunlight at 0.86 μm (Kaufman et al., 2005). Figure 8d shows that the slope of linear regression of CTP against AOD is much stronger for smoke aerosol than that for polluted aerosol, with a correlation coefficient equal to 0.36. Both these results may be due to the higher absorption efficiency of smoke (Small et al., 2011).

3.3.3 Influence of relative humidity on ACI

Feingold et al. (2001) reported that the aerosol indirect effect depends highly on the aerosol hygroscopicity and PVV. Wang et al. (2014) demonstrated that the observed interaction between aerosol and cloud can be affected by the dynamical and thermodynamical processes in cloud systems. Therefore, to explore the meteorological impact on the interaction between aerosol and cloud observed over the YRD, we classify the data for various meteorological parameters, including relative humidity (this section), LTS and PVV (Sect. 3.3.4).

Relative humidity is one of the main factors affecting aerosol particle size and cloud formation. For instance, high relative humidity at cloud base has been reported to affect the relation between aerosol particles and cloud properties (Small et al., 2011). Thus, effects of relative humidity need to be accounted for in ACI studies, as reported in the literature (Jeong et al., 2007; Loeb and Manalo-Smith, 2005; Quaas et al., 2010).

The cloud properties versus AOD relationships are classified by relative humidity (at 950 hPa) in three equally sized subsets and the mean relative humidity values for each subset are calculated. In Fig. 9 we show cloud properties as a function of AOD for only the lowest relative humidity (31 %), representing dry conditions, and the highest relative humidity (91 %, above the deliquescence point of ambient particles). Figure 9a shows that the CDR is larger in high relative humidity conditions than in low relative humidity conditions, irrespective of the AOD. It is likely that hygroscopic aerosols grow in size caused by condensation of water vapour (Hanel, 1976; Feingold et al., 2003). The increasing relative humidity further increases the probability of the cloud droplet activation and growth of existing cloud droplets as well (Jones et al., 2009). This indicates that high relative humidity conditions can help the formation of larger cloud droplets due to a higher water vapour content in the atmosphere. The cloud fraction is much larger in high relative humidity conditions than in low relative humidity conditions, as shown in Fig. 9b. Figure 9c shows that the COT decreases

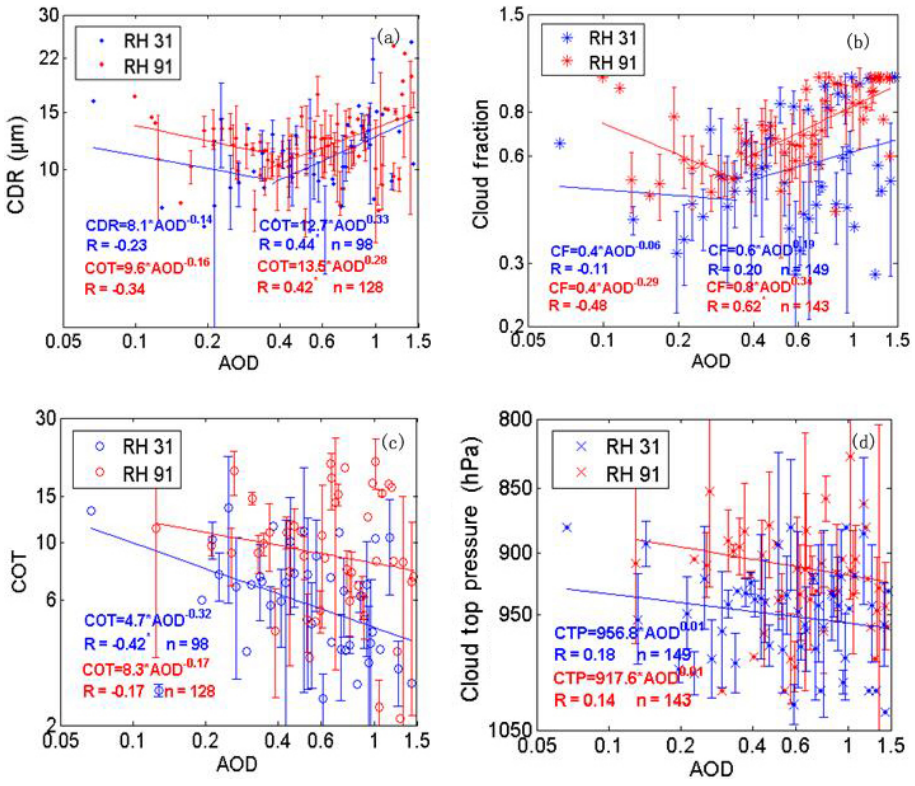

Figure 9. Scatter plots of cloud parameters versus AOD over YRD on log–log scale for cases of low relative humidity (31 %) condition (blue) and mixed aerosol–cloud layers under high relative humidity (91 %) condition (red): **(a)** CDR, **(b)** CF, **(c)** COT and **(d)** CTP. The lines present the least-square fits, and the resulting relations are presented in each figure. The error bars indicate the statistical uncertainties as in Fig. 6.

with increasing AOD in both conditions, albeit with a low significance as indicated by the small correlation coefficient R. However, the COT is larger in high relative humidity conditions than in low relative humidity conditions for the entire AOD dataset. In contrast, the CTP is smaller in high relative humidity conditions than in low relative humidity conditions over the whole range of AOD values (Fig. 9d). This implies that high relative humidity can promote the formation of thicker and higher clouds.

3.3.4 Influence of boundary layer thermodynamics and dynamics on ACI

The LTS is an indicator for the mixing state of the atmospheric layer adjacent to the surface. It describes to some extent the atmosphere's tendency to promote or suppress vertical motion (Medeiros and Stevens, 2011), which in turn affects cloud properties (Klein and Hartmann, 1993).

Figure 10 shows cloud properties as a function of AOD for two different LTS conditions: low LTS, with a mean value equal to 10.11 representing an unstable atmosphere; and high LTS, with a mean value equal to 20.47 representing a stable atmosphere. Figure 10a shows that the CDR is larger in unstable atmospheric conditions than in stable conditions, irrespective of the AOD. This indicates that in unstable atmospheric conditions the cloud droplets are larger, which may be due to stronger interaction between aerosols and clouds as a result of better vertical mixing of water vapour. Figure 10b shows that the slope of linear regression of cloud fraction against AOD is much stronger for stable atmospheric conditions than for unstable atmospheric conditions in the heavily polluted conditions. This demonstrates that stable atmospheric conditions can promote the formation of a cloud (Small et al., 2011). A high LTS indicates a strong inversion, which prevents vertical mixing and cloud vertical extent, maintaining a well-mixed and moist boundary layer and providing an environment which favours the development of a low cloud cover. Figure 10c shows that the COT is larger in unstable atmospheric conditions than in stable atmospheric conditions. In contrast, the CTP is smaller in unstable atmospheric conditions than in stable atmospheric conditions for the whole range of AOD values (Fig. 9d). This indicates that unstable atmospheric conditions can promote the formation of thicker and higher clouds and stable atmospheric conditions can enhance the cloud cover.

The PVV, a measure of dynamic convection strength, is very important for cloud formation. In particular, the vertical velocity can be used to determine whether a certain re-

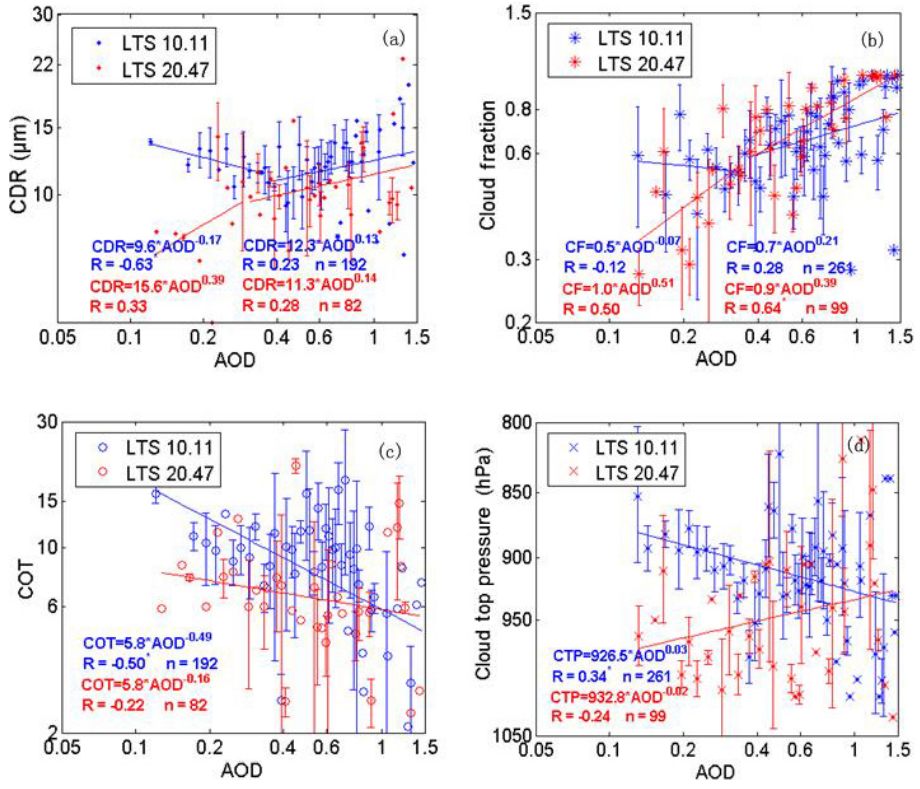

Figure 10. Scatter plots of cloud parameters versus AOD over YRD on log–log scale for cases of low LTS condition (blue) and mixed aerosol–cloud layers under high LTS condition (red): **(a)** CDR, **(b)** CF, **(c)** COT and **(d)** CTP. The lines present the least-square fits, and the resulting relations are presented in each figure. The error bars indicate the statistical uncertainties as in Fig. 6.

gion may be susceptible to cloud development or not. That is, the presence of upward motion, as indicated by negative PVV, can enhance ACI as it makes the ambient environment favourable for cloud formation, and vice versa (Jones et al., 2009).

Figure 11a shows that in moderately polluted conditions the CDR is larger in the presence of upward motion of air parcels than for downward motion. This observation indicates that the upward motion of air parcels can promote the formation of larger cloud droplets, thus enhancing ACI. However, the impact of vertical velocity is weak in polluted and heavily polluted conditions. Figure 11b shows that the cloud fraction is larger in the presence of upward motion of air parcels than for downward motion of air parcels when AOD is greater than 0.35. This indicates that the upward motion of air parcels can favour cloud development and increase cloud cover in heavily polluted conditions. The phenomenon is not obvious when AOD is smaller than 0.35. These results emphasize the importance of vertical velocity when estimating the potential aerosol effect on cloud droplet effective radius and cloud fraction. Figure 11c shows that the COT is larger in the presence of upward motion of air parcels than for downward motion throughout the range of AOD. In contrast, the CTP is smaller in the presence of upward motion of air parcels than for downward motion (Fig. 9d). This implies that upward motion of air parcels can be helpful for the formation of thicker and higher clouds.

3.4 Error sources and uncertainties

Caution is warranted in investigating the satellite-derived relations between aerosol and cloud properties. Uncertainties in satellite data may result from assumptions on the aerosol size distribution used in the retrieval process, imperfect cloud detection resulting in residual clouds leading to high AOD values, effects of relative humidity on aerosol parameters and dynamic effects (Yuan et al., 2008). Below we discuss several potential factors that may have affected the interaction between aerosols and clouds in our analysis.

Firstly, the correlation between AOD and cloud parameters may be influenced by aerosol size distributions (Small et al., 2011). Since the MODIS retrieval does not provide aerosol size information, it is better to explore the seasonal differences in the observed ACI due to the difference in aerosol emissions between the different seasons. However, the relatively low number of MODIS–CALIPSO coincidences limits the further binning of the data required to investigate this issue. Secondly, when it comes to the occurrence of cloud contamination in the AOD dataset, this is a universal and one

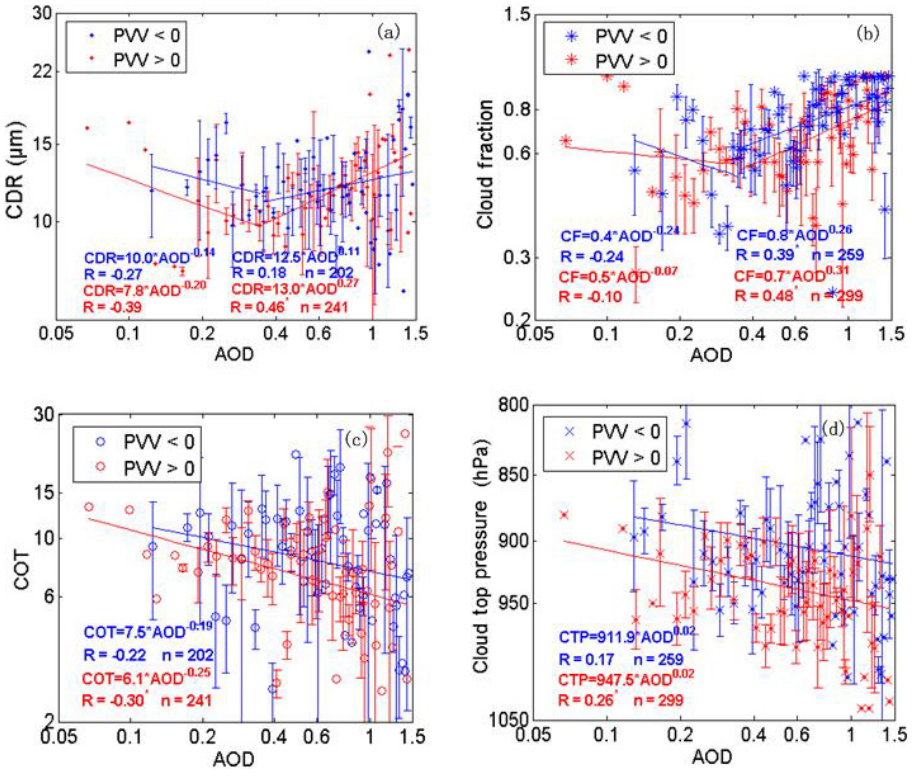

Figure 11. Scatter plots of cloud parameters versus AOD over YRD on log–log scale for cases of PVV < 0 condition (blue) and mixed aerosol–cloud layers under high PVV > 0 condition (red): **(a)** CDR, **(b)** CF, **(c)** COT and **(d)** CTP. The lines present the least-square fits, and the resulting relations are presented in each figure. The error bars indicate the statistical uncertainties as in Fig. 6.

of the most difficult problems in aerosol retrieval. Cloud detection is usually not perfect, so that undetected, or residual, clouds contaminate the retrieval area, which leads to AOD overestimation and in turn affects the relation between aerosol and cloud properties (e.g. Sogacheva et al., 2017). A study by Mei et al. (2016), comparing their MERIS cloud mask with two independent datasets, shows that of the order of 70–90 % of the cases are correctly classified as cloud-free. This result is in good agreement with that from a dedicated study on a consistency between aerosol and cloud retrievals from the same instrument, which showed that about 20 % of the pixels may be misclassified (Klueser, 2014). In this study, the samples with AOD values greater than 1.5 were excluded in a rough attempt to exclude cloud-contaminated AOD to reduce the uncertainty in the observed ACI. Thirdly, Feingold et al. (2003) reported that water vapour swelling increases the AOD. Sheridan et al. (2001) showed an important role of hygroscopic growth in determining the AOD for sea salt aerosols. The effect of humidity on the ACI has been discussed in Sect. 3.3.3. Finally, Young (1993) reported that ACI is influenced by dynamics through modifying radiative and thermodynamic heating. Jones et al. (2009) emphasized the importance of vertical mixing velocity in cloud formation and ACI as discussed in Sects. 3.3.4 and 3.3.5. As reported by Yuan et al. (2008), the potential artefacts mentioned above do not seem to be the primary cause for the observed relationship between aerosol and cloud parameters. Further investigations are needed to fully analyse and explain the observed phenomena.

4 Conclusions

The high level of anthropogenic emissions in eastern China render this area an important hotspot for studying how cloud micro-physical properties are affected by anthropogenic aerosols (Ding et al., 2013b). Based on the near-simultaneous aerosol and cloud retrievals provided by MODIS, CALIOP and CloudSat, together with the ERA-Interim reanalysis data, we investigated the effect of aerosols, with AOD used as a proxy for the aerosol loading, on micro-physical and macro-physical cloud properties over the YRD for the years 2007 to 2010. In terms of the relative heights of aerosol and cloud layers, well-mixed and separated clouds were defined. A statistical analysis was used to examine the aerosol effects on cloud properties for these two cases. Besides the aerosol impact on CDR, CF, COT and CTP, the influence of environmental conditions, such as relative humidity, LTS and PVV, on the relation between cloud properties and AOD was also

studied. In addition, the impact of two different aerosol types, dust and smoke, was explored.

The analysis of the COT–CDR and CWP–CDR relationships for well-mixed clouds indicated that they are affected by the aerosol loading. A statistical analysis of the relation between CWP and COT showed an increase in CWP with an increasing COT, which is in a good agreement with the findings reported by Costantino and Bréon (2013).

Consistent with previous findings, we found that the CDR initially decreases with increasing AOD, followed by an increase after AOD reaches a value of 0.35. This result is consistent with Twomey's hypothesis that increasing aerosol abundance leads to more numerous but smaller cloud droplets at given constant cloud water content. The positive relation between CDR and AOD may be caused by microphysical processes, which is coupled with intense vapour competition and evaporation of smaller droplets as a result of a high abundance of aerosol particles. Also, the analysis of the variation of CF with increasing AOD showed that CF varies with AOD in a way similar to that of CDR. This finding differs from those by Koren et al. (2008) and Small et al. (2011) who observed an increase in the cloud cover with an increasing AOD, followed by a decrease with higher AOD. COT was found to decrease with an increasing AOD. We argue that the radiative effect and retrieval artefact due to absorbing aerosol might be important factors in determining this relationship. This effect can result in increased cloud evaporation and reduced cloud cover. Meanwhile, CTP tends to increase as aerosol abundance increases, indicating that the aerosol is prone to expanding the horizontal extension. In other words, we found that for well-mixed clouds over the YRD, the CDR becomes smaller with the increase of AOD in moderately polluted conditions, which is, in principle, in line with the Twomey effect, yet the cloud fraction indicates a weak decrease which could be attributed only to the weak influence of evaporation caused by absorption of aerosols.

On the other hand, in polluted and heavily polluted conditions, a reduced cloud coverage can result in more solar radiation reaching the surface, causing surface heating and thus raising the surface temperature, which then destabilizes the atmosphere. The resulting advection transports water vapour from the surface to higher levels in the atmosphere, therefore producing more cloud. Meanwhile, CDR becomes larger as a result of the stronger water vapour competition in polluted and heavily polluted conditions. The COT decreases with the increasing values of AOD throughout the AOD range due to the radiative effect and possible retrieval artefacts. The behaviour of CTP is consistent with that of COT, with the cloud getting thinner but with larger cover, so that CTP becomes larger with an increasing AOD.

Furthermore, joint correlative analysis of different aerosol and cloud properties revealed that smoke aerosols have a stronger impact on ACI due to their stronger absorption of solar radiation compared with polluted dust. Therefore, we can conclude that absorbing aerosols play an important role in the ACI.

Constrained by relative humidity and boundary thermodynamic and dynamic conditions, the variation of cloud properties in response to aerosol abundance was analysed. In general, a high relative humidity can promote the formation of larger cloud droplets and expand cloud formation, irrespective of the vertical or horizontal level. With regard to LTS, stable atmospheric conditions can enhance the cloud cover horizontally. However, unstable atmospheric conditions can be helpful for the formation of thicker and higher clouds. Dynamically, an upward motion of air parcels can also facilitate the formation of thicker and higher clouds. Besides the meteorological controls mentioned above, other factors may be important in generating relations between aerosol and cloud properties, such as temperature advection. These results suggest that effects of ambient meteorological environments need to be considered when exploring the aerosol indirect effect. In summary, this study will greatly help us to understand the mechanisms of ACI and ultimately of indirect aerosol effects over the YRD.

Data availability. All data used in this study are publicly available. The satellite data from the MODIS instrument used in this study were obtained from https://ladsweb.nascom.nasa.gov/search/ (Liu, 2015a). The satellite data from CloudSat were obtained from http://www.cloudsat.cira.colostate.edu/order-data/ (Liu, 2015b). The satellite data from CALIOP were obtained from https://www-calipso.larc.nasa.gov/tools/data_avail/ (Liu, 2015c). The ECMWF ERA-Interim data were collected from the ECMWF data server http://apps.ecmwf.int/datasets/data/interim-full-daily/levtype=pl/ (Liu, 2016).

Competing interests. The authors declare that they have no conflict of interest.

Acknowledgements. This work was supported by the National Key Research and Development Program of China (no. 2016YFD0300101), the 1–3–5 Innovation Project of RADI_CAS (no. Y3ZZ15101A), the National Natural Science Foundation of China (no. 31571565), Open Fund of Key Laboratory of ULRMS, MLR (no. KF-2016-02-026) and FCoE, Academy Professorship. We are grateful to the ease access to MODIS, CALIPSO and CloudSat, provided by NASA and CNES. We also thank ECMWF for providing daily ERA-Interim reanalysis data in our work.

Edited by: I. Salma
Reviewed by: two anonymous referees

References

Alam, K., Khan, R., Blaschke, T., and Mukhtiar, A.: Variability of aerosol optical depth and their impact on cloud properties in Pakistan, J. Atmos. Sol.-Terr. Phy., 107, 104–112, 2014.

Albrecht, B. A.: Aerosols, cloud microphysics, and fractional cloudiness, Science, 245, 4923, 1227–1230, 1989.

Andersson, A., Deng, J., Du, K., Zheng, M., Yan, C., Sköld, M., and Gustafsson, O.: Regionally-varying combustion sources of the January 2013 severe haze events over eastern China, Environ. Sci. Technol., 49, 2038–2043, doi:10.1021/es503855e, 2015.

Andreae, M. O.: Correlation between cloud condensation nuclei concentration and aerosol optical thickness in remote and polluted regions, Atmos. Chem. Phys., 9, 543–556, doi:10.5194/acp-9-543-2009, 2009.

Cao, Q., Yu, D., Georgescu, M., and Wu, J.: Impacts of urbanization on summer climate in China: An assessment with coupled land-atmospheric modeling, J. Geophys. Res.-Atmos., 121, 10505–10521, doi:10.1002/2016JD025210, 2016.

Costantino, L. and Bréon, F.-M.: Analysis of aerosol-cloud interaction from multi-sensor satellite observations, Geophys. Res. Lett., 37, L11801, doi:10.1029/2009GL041828, 2010.

Costantino, L. and Bréon, F.-M.: Aerosol indirect effect on warm clouds over South-East Atlantic, from co-located MODIS and CALIPSO observations, Atmos. Chem. Phys., 13, 69–88, doi:10.5194/acp-13-69-2013, 2013.

Ding, A. J., Fu, C. B., Yang, X. Q., Sun, J. N., Zheng, L. F., Xie, Y. N., Herrmann, E., Nie, W., Petäjä, T., Kerminen, V.-M., and Kulmala, M.: Ozone and fine particle in the western Yangtze River Delta: an overview of 1 yr data at the SORPES station, Atmos. Chem. Phys., 13, 5813–5830, doi:10.5194/acp-13-5813-2013, 2013a.

Ding, A. J., Fu, C. B., Yang, X. Q., Sun, J. N., Petäjä, T., Kerminen, V.-M., Wang, T., Xie, Y., Herrmann, E., Zheng, L. F., Nie, W., Liu, Q., Wei, X. L., and Kulmala, M.: Intense atmospheric pollution modifies weather: a case of mixed biomass burning with fossil fuel combustion pollution in eastern China, Atmos. Chem. Phys., 13, 10545–10554, doi:10.5194/acp-13-10545-2013, 2013b.

Duesk, U., Frank, G. P., Hildebrandt, L., Curtius, J., Schneider, J., Walter, S., Chand, D., Drewnick, F., Hings, S., Jung, D., Borrmann, S., and Andreae, M. O.: Size matters more than chemistry for cloud-nucleating ability of aerosol particles, Science, 312, 1375–1378, 2006.

Feingold, G., Eberhard, W., Veron, D., and Previdi, M.: First measurements of the Twomey indirect effect using ground-based remote sensors, Geophys. Res. Lett., 30, 1287, doi:10.1029/2002GL016633, 2003.

Feingold, G., Remer, L. A., Ramaprasad, J., and Kaufman, Y. J.: Analysis of smoke impact on clouds in Brazilian biomass burning regions: an extension of Twomey's approach, J. Geophys. Res., 106, 22907–22922, 2001.

Gao, W. H., Sui, C.-H., and Hu, Z. J.: A study of macrophysical and microphysical properties of warm clouds over the Northern Hemisphere using CloudSat/CALIPSO data, J. Geophys. Res., 119, 3268–3280, doi:10.1002/2013JD020948, 2014.

Grandey, B. S. and Stier, P.: A critical look at spatial scale choices in satellite-based aerosol indirect effect studies, Atmos. Chem. Phys., 10, 11459–11470, doi:10.5194/acp-10-11459-2010, 2010.

Gryspeerdt, E., Stier, P., and Partridge, D. G.: Satellite observations of cloud regime development: the role of aerosol processes, Atmos. Chem. Phys., 14, 1141–1158, doi:10.5194/acp-14-1141-2014, 2014.

Gryspeerdt, E., Quaas, J., and Bellouin, N.: Constraining the aerosol influence on cloud fraction, J. Geophys. Res., 121, 3566–3583, 2016.

Hanel, G.: The properties of atmospheric aerosol particles as function of the relative humidity at thermodynamic equilibrium with the surrounding moist air, Adv. Geophys., 19, 73–188, 1976.

Im, E., Wu, C. L., and Durden, S. L.: Cloud profiling radar for the CloudSat mission, IEEE Aerosp. Electron. Syst. Mag., 20, 15–18, 2005.

Jeong, M.-J., Li, Z., Andrews, E., and Tsay, S.-C.: Effect of aerosol humidification on the column aerosol optical thickness over the Atmospheric Radiation Measurement Southern Great Plains site, J. Geophys. Res.-Atmos., 112, D10202, doi:10.1029/2006JD007176, 2007.

Jones, T. A., Christopher, S. A., and Quaas, J.: A six year satellite-based assessment of the regional variations in aerosol indirect effects, Atmos. Chem. Phys., 9, 4091–4114, doi:10.5194/acp-9-4091-2009, 2009.

Kaufman, Y. J., Remer, L. A., Tanre, D., Rong-Rong, L., Kleidman, R., Mattoo, S., Levy, R. C., Eck, T. F., Holben, B. N., Ichoku, C., Martins, J. V., and Koren, I.: A critical examination of the residual cloud contamination and diurnal sampling effects on MODIS estimates of aerosol over ocean, IEEE T. Geosci. Remote, 43, 2886–2897, doi:10.1109/TGRS.2005.858430, 2005.

Kaufman, Y. J. and Koren I.: Smoke and Pollution Aerosol Effect on Cloud Cover, Science, 313, 655–658, doi:10.1126/science.1126232, 2006.

Kaufman, Y. J., Koren, I., Remer, L. A., Rosenfeld, D., and Rudich, Y.: The effect of smoke, dust, and pollution aerosol on shallow cloud development over the Atlantic Ocean, PNAS, 102, 11207–11212, doi:10.1073/pnas.0505191102, 2012.

King, M. D., Tsay, S. C., Platnick, S. E., Wang, M., and Liou, K. N.: Cloud Retrieval Algorithms for MODIS: Optical Thickness, Effective Particle Radius, and Thermodynamic Phase, MODIS Algorithm Theoretical Basis Document, available at: http://eospso.nasa.gov/sites/default/files/atbd/atbd_mod05.pdf (last access: 27 April 2017), 1997.

King, M. D., Menzel, W. P., Kaufman, Y. J., Tanré, D., Gao, B. C., Platnick, S., Ackerman, S. A., Remer, L. A., Pincus, R., and Hubanks, P. A.: Cloud and aerosol properties, precipitable water, and profiles of temperature and water vapor from MODIS, IEEE T. Geosci. Remote, 41, 442–458, doi:10.1109/TGRS.2002.808226, 2003.

Klein, S. A. and Hartmann, D. L.: The seasonal cycle of low stratiform clouds, J. Climate., 6, 1587–1606, 1993.

Klueser, L.: ESA Climate Change Initiative: Aerosol_cci/Cloud_cci, Cloud Mask Consistency Analysis Report (joint option), Report Version 1.1, available at: http://www.esa-aerosol-cci.org/?q=webfm_send/1199, 2014.

Koren, I., Kaufman, Y. J., Rosenfeld, D., Remer, L. A., and Rudich, Y.: Aerosol invigoration and restructuring of Atlantic convective clouds, Geophys. Res. Lett., 32, L14828, doi:10.1029/2005gl023187, 2005.

Koren, I., Feingold, G., and Remer, L. A.: The invigoration of deep convective clouds over the Atlantic: aerosol effect, meteorol-

ogy or retrieval artifact?, Atmos. Chem. Phys., 10, 8855–8872, doi:10.5194/acp-10-8855-2010, 2010.

Koren, I., Martins, J. V., Remer, L. A., and Afargan, H.: Smoke invigoration versus inhabitation of clouds over the Amazon, Science, 321, 946–949, doi:10.1126/science.1159185, 2008.

Kourtidis, K., Stathopoulos, S., Georgoulias, A. K., Alexandri, G., and Rapsomanikis, S.: A study of the impact of synoptic weather conditions and water vapor on aerosol–cloud relationships over major urban clusters of China, Atmos. Chem. Phys., 15, 10955–10964, doi:10.5194/acp-15-10955-2015, 2015.

Krüger, O. and Graßl, H.: Southern Ocean phytoplankton increases cloud albedo and reduces precipitation, Geophys. Res. Lett., 38, L08809, doi:10.1029/2011GL047116, 2011.

Krüger, O. and Graßl, H.: The indirect aerosol effect over Europe, Geophys. Res. Lett., 29, 1925, doi:10.1029/2001GL014081, 2002.

Krüger, O., Marks, R., and Graßl, H.: Influence of Pollution on Cloud Reflectance, J. Geophys. Res., 109, D24210, doi:10.1029/2004JD004625, 2004.

Levin, Z., Ganor, E., and Gladstein, V.: The effects of desert particles coated with sulfate on rain formation in the eastern Mediterranean, J. Appl. Meteor., 35, 1511–1523, 1996.

Levy, R. C., Remer, L. A., Kleidman, R. G., Mattoo, S., Ichoku, C., Kahn, R., and Eck, T. F.: Global evaluation of the Collection 5 MODIS dark-target aerosol products over land, Atmos. Chem. Phys., 10, 10399–10420, doi:10.5194/acp-10-10399-2010, 2010.

Li, Z., Zhao, F., Liu, J., Jiang, M., Zhao, C., and Cribb, M.: Opposite effects of absorbing aerosols on the retrievals of cloud optical depth from spaceborne and ground-based measurements, J. Geophys. Res.-Atmos., 119, 5104–5114, doi:10.1002/2013JD021053, 2014.

Liu, Y. Q.: Institute of Remote Sensing and Digital Earth, Chinese Academy of Sciences, MODIS Atmosphere Level-2 Daily Product, available at: https://ladsweb.nascom.nasa.gov/search/, last access: 22 December 2015a.

Liu, Y. Q.: Institute of Remote Sensing and Digital Earth, Chinese Academy of Sciences, the latest version (R04) of the CloudSat standard data products, available at: https://www.cloudsat.cira.colostate.edu/order-data/, last access: 26 December 2015b.

Liu, Y. Q.: Institute of Remote Sensing and Digital Earth, Chinese Academy of Sciences, CALIOP Level-2 aerosol layers product, available at: https://www-calipso.larc.nasa.gov/tools/data_avail/, last access: 28 December 2015c.

Liu, Y. Q.: Institute of Remote Sensing and Digital Earth, Chinese Academy of Sciences, ERA-Interim reanalysis data set, available at: http://apps.ecmwf.int/datasets/data/interim-full-daily/levtype=pl/, last access: 28 March 2016.

Liu, Z., Vaughan, M., Winker, D., Kittaka, C., Getzewich, B., Kuehn, R., Omar, A.,Powell, K., Trepte, C., and Hostetler, C.: The CALIPSO lidar cloud and aerosol discrimination: Version 2 algorithm and initial assessment of performance, J. Atmos. Ocean. Tech., 26, 1198–1213, 2009.

Loeb, N. G. and Manalo-Smith, N.: Top-of-atmosphere direct radiative effect of aerosols over global oceans from merged CERES and MODIS observations, J. Climate, 18, 3506–3526, 2005.

Loeb, N. G. and Schuster, G. L.: An observational study of the relationship between cloud, aerosol and meteorology in broken low-level cloud conditions, J. Geophys. Res.-Atmos., 113, D14214, doi:10.1029/2007JD009763, 2008.

Matheson, M. A., Coakley Jr., J. A., and Tahnk, W. R.: Aerosol and cloud property from relationships for summer stratiform clouds in the northeastern Atlantic from advanced very high resolution radiometer observations, J. Geophys. Res., 110, D24204, doi:10.1029/2005JD006165, 2005.

Matrosov, S. Y.: Potential for attenuation-based estimations of rainfall rate from CloudSat, Geophys. Res. Lett., 34, L05817, doi:10.1029/2006GL029161, 2007.

Matsui, T., Masunaga, H., Kreidenweis, S. M., Pielke Sr., R. A., Tao, W.-K., Chin, M., and Kaufman, Y. J.: Satellite based assessment of marine low cloud variability associated with aerosol, atmospheric stability, and the diurnal cycle, J. Geophys. Res., 111, D17204, doi:10.1029/2005JD006097, 2006.

McCormick, R. A. and Ludwig, J. H.: Climate modification by atmospheric aerosols, Science, 156, 1358–1359, 1967.

Medeiros, B. and Stevens, B.: Revealing differences in GCM representations of low clouds, Clim. Dynam., 36, 385–399, 2011.

Mei, L., Vountas, M., Gómez-Chova, L., Rozanov, V., Jäger, M., Lotz, W., Burrows, J. P., and Hollmann, R.: A Cloud masking algorithm for the XBAER aerosol retrieval using MERIS data, Remote Sens. Environ., doi:10.1016/j.rse.2016.11.016, 2016.

Menon, S., Del Genio, A. D., Kaufman, Y., Bennartz, R., Koch, D., Loeb, N., and Orlikowski, D.: Analysis signatures of aerosol-cloud interactions from satellite retrievals and the GISS GCM to constrain the aerosol indirect effect, J. Geophys. Res.-Atmos., 113, D14S22, doi:10.1029/2007jd009442, 2008.

Meskhidze, N. and Nenes, A.: Effects of ocean ecosystem on marine aerosol-cloud interaction, Adv. Meteorol., 2010, 239808, doi:10.1155/2010/239808, 2010.

Meyer, K., Platnick, S., Oreopoulos, L., and Lee, D.: Estimating the direct radiative effect of absorbing aerosols overlying marine boundary layer clouds in the southeast Atlantic using MODIS and CALIOP, J. Geophys. Res., 118, 4801–4815, doi:10.1002/jgrd.50449, 2013.

Meyer, K., Platnick, S., and Zhang, Z.: Simultaneously inferring above-cloud absorbing aerosol optical thickness and underlying liquid phase cloud optical and microphysical properties using MODIS, J. Geophys. Res.-Atmos., 120, 5524–5547, doi:10.1002/2015JD023128, 2015.

Michibata, T., Kawamoto, K., and Takemura, T.: The effects of aerosols on water cloud microphysics and macrophysics based on satellite-retrieved data over East Asia and the North Pacific, Atmos. Chem. Phys., 14, 11935–11948, doi:10.5194/acp-14-11935-2014, 2014.

Nie, W., Ding, A. J., Wang, T., Kerminen, V.-M., George, C., Xue, L. K., Wang, W. X., Zhang, Q. Z., Petäjä, T., Qi, X. M., Gao, X. M., Wang, X. F., Yang, X. Q., Fu, C. B., and Kulmala, M.: Polluted dust promotes new particle formation and growth, Scientific Reports, 4, 6634, doi:10.1038/srep06634, 2014.

Patra, P. K., Behera, S. K., Herman, J. R., Maksyutov, S., Akimoto, H., and Yamagata, Y.: The Indian summer monsoon rainfall: interplay of coupled dynamics, radiation and cloud microphysics, Atmos. Chem. Phys., 5, 2181–2188, doi:10.5194/acp-5-2181-2005, 2005.

Platnick, S., King, M. D., Ackerman, S. A., Menzel, W. P., Baum, B. A., Riedi, J. C., and Frey, R. A.: The MODIS cloud products: algorithms and examples from Terra, IEEE T. Geosci. Remote, 41, 459–473, 2003.

Qi, X. M., Ding, A. J., Nie, W., Petäjä, T., Kerminen, V.-M., Herrmann, E., Xie, Y. N., Zheng, L. F., Manninen, H., Aalto, P., Sun, J. N., Xu, Z. N., Chi, X. G., Huang, X., Boy, M., Virkkula, A., Yang, X.-Q., Fu, C. B., and Kulmala, M.: Aerosol size distribution and new particle formation in the western Yangtze River Delta of China: 2 years of measurements at the SORPES station, Atmos. Chem. Phys., 15, 12445–12464, doi:10.5194/acp-15-12445-2015, 2015.

Quaas, J., Ming, Y., Menon, S., Takemura, T., Wang, M., Penner, J. E., Gettelman, A., Lohmann, U., Bellouin, N., Boucher, O., Sayer, A. M., Thomas, G. E., McComiskey, A., Feingold, G., Hoose, C., Kristjánsson, J. E., Liu, X., Balkanski, Y., Donner, L. J., Ginoux, P. A., Stier, P., Grandey, B., Feichter, J., Sednev, I., Bauer, S. E., Koch, D., Grainger, R. G., Kirkevåg, A., Iversen, T., Seland, Ø., Easter, R., Ghan, S. J., Rasch, P. J., Morrison, H., Lamarque, J.-F., Iacono, M. J., Kinne, S., and Schulz, M.: Aerosol indirect effects – general circulation model intercomparison and evaluation with satellite data, Atmos. Chem. Phys., 9, 8697–8717, doi:10.5194/acp-9-8697-2009, 2009.

Quaas, J., Stevens, B., Stier, P., and Lohmann, U.: Interpreting the cloud cover – aerosol optical depth relationship found in satellite data using a general circulation model, Atmos. Chem. Phys., 10, 6129–6135, doi:10.5194/acp-10-6129-2010, 2010.

Ramanathan, V., Ctzen, P. J., Kiehl, J. T., and Rosenfeld, D.: Aerosols, climate, and the hydrological cycle, Science, 294, 2119–2124, 2001.

Remer, L. A., Kaufman, Y. J., Tanre, D., Mattoo, S., Chu, D. A., Martins, J. V., Li, R. R., Ichoku, C., Levy, R. C., Kleidman, R. G., Eck, T. F., Vermote, E., and Holben, B. N.: The MODIS aerosol algorithm, products, and validation, J. Atmos. Sci., 62, 947–973, doi:10.1175/JAS3385.1, 2005.

Rennó, N. O., Williams, E., Rosenfeld, D., Fischer, D. G., Fischer, J. R., Kremic, T., Agrawal, A., Andreae, M. O., Bierbaum, R., Blakeslee, R., Boerner, A., Bowles, N., Christian, H., Cox, A., Dunion, J., Horvath, A., Huang, X., Khain, A., Kinne, S., Lemos, M. C., Penner, J. E., Pöschl, U., Quaas, J., Seran, E., Stevens, B., Walati, T., and Wagner, T.: CHASER: an innovative satellite mission concept tomeasure the effects of aerosols on clouds and climate, B. Am. Meteorol. Soc., 94, 685–694, 2013.

Reutter, P., Su, H., Trentmann, J., Simmel, M., Rose, D., Gunthe, S. S., Wernli, H., Andreae, M. O., and Pöschl, U.: Aerosol- and updraft-limited regimes of cloud droplet formation: influence of particle number, size and hygroscopicity on the activation of cloud condensation nuclei (CCN), Atmos. Chem. Phys., 9, 7067–7080, doi:10.5194/acp-9-7067-2009, 2009.

Rosenfeld, D.: Suppression of rain and snow by urban and industrial air pollution, Science, 287, 1793–1796, 2000.

Rosenfeld, D., Andreae, M. O., Asmi, A., Chin, M., de Leeuw, G., Donovan, D., Kahn, R., Kinne, S., Kivekäs, N., Kulmala, M., Lau, W., Schmidt, S., Suni, T., Wagner, T., Wild, M., and Quaas, J.: Global observations of aerosol-cloud-precipitation-climate interactions, Rev. Geophys., 52, 750–808, doi:10.1002/2013RG000441, 2014.

Saponaro, G., Kolmonen, P., Sogacheva, L., Rodriguez, E., Virtanen, T., and de Leeuw, G.: Estimates of the aerosol indirect effect over the Baltic Sea region derived from 12 years of MODIS observations, Atmos. Chem. Phys., 17, 3133–3143, doi:10.5194/acp-17-3133-2017, 2017.

Satheesh, S. K., Moorthy, K. K., Kaufman, Y. J., and Takemura, T.: Aerosol optical depth, physical proper ties and radiative forcing over the Arabian Sea, Meteorol. Atmos. Phys., 91, 45–62, 2006.

Sena, E. T., McComiskey, A., and Feingold, G.: A long-term study of aerosol-cloud interactions and their radiative effect at the Southern Great Plains using ground-based measurements, Atmos. Chem. Phys., 16, 11301–11318, doi:10.5194/acp-16-11301-2016, 2016.

Sinha, P., Hobbs, P. V., Yokelson, R. J., Blake, D. R., Gao, S., and Kirchstetter, T. W.: Distributions of trace gases and aerosols during the dry biomass burning season in southern Africa, J. Geophys. Res., 108, 4536, doi:10.1029/2003JD003691, 2003.

Small, J. D., Jiang, J. H., Su, H., and Zhai, C.: Relationship between aerosol and cloud fraction over Australia, Geophys. Res. Lett., 38, L23802, doi:10.1029/2011GL049404, 2011.

Sogacheva, L., Kolmonen, P., Virtanen, T. H., Rodriguez, E., Saponaro, G., and de Leeuw, G.: Post-processing to remove residual clouds from aerosol optical depth retrieved using the Advanced Along Track Scanning Radiometer, Atmos. Meas. Tech., 10, 491–505, doi:10.5194/amt-10-491-2017, 2017.

Sporre, M. K., Swietlicki, E., Glantz, P., and Kulmala, M.: A long-term satellite study of aerosol effects on convective clouds in Nordic background air, Atmos. Chem. Phys., 14, 2203–2217, doi:10.5194/acp-14-2203-2014, 2014.

Stathopoulos, S., Georgoulias, A. K., and Kourtidis, K.: Spaceborne observations of aerosol-cloud relations for cloud systems of different heights, Atmos. Res., 183, 191–201, 2017.

Stephens, G., Vane, D. G., Boain, R. J., Mace, G. G., Sassen, K., Wang, Z., Illingworth, A. J., O'Connor, E. J., Rossow, W. B., Durden, S. L., Miller, S. D., Austin, R. T., Benedetti, A., and Mitrescu, C.: The CloudSat Science Team: The CloudSat mission and the A-Train, B. Am. Meteorol. Soc., 83, 1771–1790, 2002.

Stevens, B. and Feingold, G.: Untangling aerosol effects on clouds and precipitation in a buffered system, Nature, 461, 607–613, doi:10.1038/nature08281, 2009.

Su, W., Loeb, N. G., Xu, K.-M., Schuster, G. L., and Eitzen, Z. A.: An estimate of aerosol indirect effect from satellite measurements with concurrent meteorological analysis, J. Geophys. Res.-Atmos., 115, D18219, doi:10.1029/2010JD013948, 2010.

Sundström, A.-M., Kolmonen, P., Sogacheva, L., and de Leeuw, D.: Aerosol retrievals over China with the AATSR dual view algorithm, Remote Sens. Environ., 116, 189–198, 2012.

Suzuki, K., Nakajima, T., Numaguti, A., Takemura, T., Kawamoto, K., and Higurashi, A.: A study of the aerosol effect on a cloud field with simultaneous use of GCM modeling and satellite observation, J. Atmos. Sci., 61, 179–194, 2004.

Tang, J., Wang, P., Mickley, L. J., Xia, X., Liao, H., Yue, X., Sun, L., and Xia, J.: Positive relationship between liquid cloud droplet effective radius and aerosol optical depth over Eastern China from satellite data, Atmos. Environ., 84, 244–253, 2014.

Ten Hoeve, J. E., Remer, L. A., and Jacobson, M. Z.: Microphysical and radiative effects of aerosols on warm clouds during the Amazon biomass burning season as observed by MODIS: impacts of water vapor and land cover, Atmos. Chem. Phys., 11, 3021–3036, doi:10.5194/acp-11-3021-2011, 2011.

Twomey, S.: Pollution and the planetary albedo, Atmos. Environ., 41, 120–125, 1974.

Twomey, S.: The influence of pollution on the shortwave albedo of clouds, J. Atmos. Sci., 34, 1149–1152, 1977.

Wang, Z., Vane, D., Stephens, G., and Reinke, D.: CloudSat Project: Level 2 Combined Radar and Lidar Cloud Scenario Classification Product Process Description and Interface Control Document, 61 pp., California Institute of Technology, Calif, 2013.

Wang, F., Guo, J., Zhang, J., Wu, Y., Zhang, X., Deng, M., and Li, X.: Satellite observed aerosol-induced variability in warm cloud properties under different meteorological conditions over eastern China, Atmos. Environ., 84, 122–132, 2014.

Wang, F., Guo, J., Zhang, J., Huang, J., Min, M., Chen, T., Liu, H., Deng, M., and Li, X.: Multi-sensor quantification of aerosol-induced variability in warm clouds over eastern China, Atmos. Environ., 113, 1–9, 2015.

Winker, D. M., Pelon, J. R., and McCormick, M. P.: The CALIPSO mission: Spacebornelidar for observation of aerosols and clouds, Proc. SPIE, Lidar Remote Sensing for Industry and Environment Monitoring III, 4893, doi:10.1117/12.466539, 2003.

Yuan, T., Li, Z., Zhang, R., and Fan, J.: Increase of cloud droplet size with aerosol optical depth: an observation and modeling study, J. Geophys. Res., 113, D04201, doi:10.1029/2007JD008632, 2008.

Zhang, N., Gao, Z., Wang, X., and Chen, Y.: Moedling the impact of urbanization on the local and regional climate in Yangtze River Delta, China, Theor. Appl. Climatol., 102, 331–342, 2010.